

Article

Hydrogen from Radiolysis of Aqueous Fluid Inclusions during Diagenesis

John Parnell ^{1,*} and Nigel Blamey ^{1,2,3}

¹ School of Geosciences, University of Aberdeen, Aberdeen AB24 3UE, UK

² Department of Earth Sciences, Brock University, 500 Glenridge Avenue, St. Catharines, ON L2S 3A1, Canada; nblamey@brocku.ca

³ Department of Earth Sciences, Western University, London, ON N6A 5B7, Canada

* Correspondence: J.Parnell@abdn.ac.uk; Tel.: +44-1224-273-464

Received: 24 May 2017; Accepted: 19 July 2017; Published: 25 July 2017

Abstract: A suite of Permian sylvite samples from Boulby potash mine, Yorkshire, UK, consistently yield traces of hydrogen upon analysis by a cold crush technique for liberating volatiles from entrapped fluid inclusions. In contrast, accompanying halite samples do not yield hydrogen. These data suggest the formation of hydrogen by radiolysis of water due to irradiation from potassium in the sylvite. The data indicate radiolysis as a mechanism for subsurface hydrogen generation, where it is available as an electron donor for a deep biosphere.

Keywords: fluid inclusions; hydrogen; sylvite; halite; boulby mine; deep biosphere; radiolysis

1. Introduction

The most common liquid entrapped in fluid inclusions is water, representing the most widespread ambient fluid in the upper crust. The water may be modified relative to its original composition, due to crystallization of dissolved salts, interaction with the host mineral, or leakage. However, in some circumstances, the water may be broken down into its constituent hydrogen and oxygen. This can be the consequence of radiolysis, involving the dissociation of water due to irradiation. This is most evident in uranium ores, where intense irradiation can lead to the formation of discrete volumes of hydrogen and oxygen in aqueous fluid inclusions [1,2]. This conspicuous consequence of radiolysis in highly radioactive ores implies that lesser amounts of hydrogen and oxygen would form in rocks containing lesser amounts of uranium or thorium, or potassium.

The possibility of hydrogen generation in potassium-bearing rocks is especially significant in the potash ore mineral sylvite (potassium chloride, KCl). Like the sodium mineral equivalent halite (NaCl), sylvite contains abundant and relatively large aqueous inclusions (Figure 1). The combination of high potassium content and high water content in sylvite could result in the generation of measurable quantities of hydrogen. This potential is realized in potash ore deposits.

Previous research, especially in the U.S.S.R., has shown that hydrogen occurs in potassium evaporites, especially the chloride minerals sylvite and carnallite, and concluded that the hydrogen is a consequence of radiolysis [3,4]. More generally, hydrogen and helium in deep groundwaters may reflect long-term radiolysis [5,6].

Previous measurements have been made on bulk potash ores. Modern techniques allow measurements on individual mineral samples. In this study, we use a cold crush technique, in which the volatiles liberated from fluid inclusions by crushing are analysed in a quadrupole mass spectrometer [7,8]. This approach, originally developed for the analysis of fluid inclusions in ore deposits and geothermal systems, has been proven to detect anomalous hydrogen generated by seismogenic deformation [9]. Previous studies have concluded that natural radiolysis from potassium would generate hydrogen that could be used as an electron donor for subsurface microbial

communities [10,11]. Sylvite is a good mineral to test hydrogen generation from radiolysis because halide minerals contain relatively abundant and large fluid inclusions, so have a high entrained water content and the fluids are thus amenable to analysis. Here we analyse sylvite samples, and halite samples as a control, from an underground potash deposit in the U.K., to test if such rocks could generate hydrogen in the subsurface.

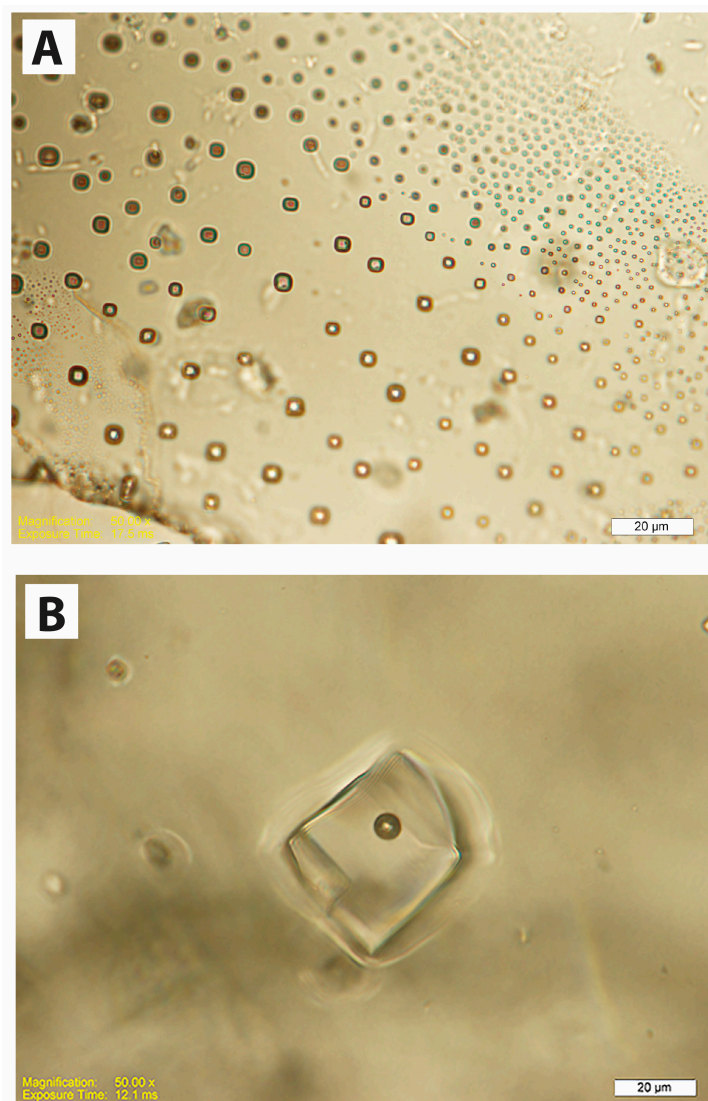


Figure 1. Photomicrographs of sylvite crystals from Boulby, showing aqueous fluid inclusions. (A) planar arrays of monophase inclusions parallel to crystal growth zones; (B) isolated inclusion with a vapour bubble. Scale bars are each 20 microns.

2. Materials and Methods

Samples were collected from the Boulby potash mine, Yorkshire, U.K., and a borehole, Eskdale No. 2, nearby at Aislaby [12] (Figure 2). The mine exploits marine evaporites of Upper Permian age (Zechstein) including thick beds of the potassium chloride sylvite [13,14]. The sylvite and halite from the Boulby mine were collected underground from stock piles accumulated from thick (>1 m) beds of relatively pure salt, rather than intergrowths of the two minerals. The mine site is used as a testing laboratory for astrobiology, including the investigation of potential habitats for life [15,16].

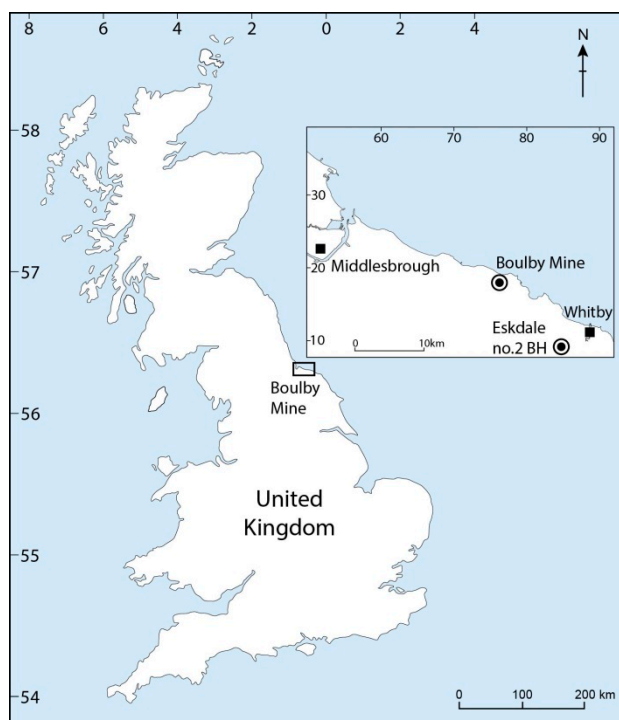


Figure 2. Map showing sample localities at Boulby potash mine and Eskdale No. 2 borehole.

Sylvite and halite were cleaned with isopropanol to remove surface organics followed by air-drying, and then placed under vacuum overnight to remove interstitial and intercrystalline gas. A sample consisted of several match head-sized mineral pieces (2–4 mm in diameter) that were crushed incrementally. The crusher is an MDC AV-075 (BMI Surplus, Inc., Hanover, MA, USA) valve with one end blanked off, leaving one opening to the mass spectrometer. The sample is placed between two metal disks and the act of incrementally closing the valve sandwiches the disks together and crushes the sample. Blanks are taken into account as described in Blamey et al. (2015); as sylvite is very soft, the blank signal is almost indistinguishable from the mass spectrometer noise. Crushes were of equal magnitude, and produced 5 to 12 successive gas bursts before crushing was completed. Data acquisition was performed with two Pfeiffer Prisma (Berlin, Germany) quadrupole mass spectrometers operating in crush-fast scan (CFS) peak-hopping mode [7,17]. The instrument was calibrated using Scott Gas Mini-mix gas mixtures (with 2% uncertainty), and verified with capillary tubes (with 1% uncertainty) filled with gas mixtures, and three in-house fluid inclusion gas standards. The amount of gas was calculated by matrix multiplication to provide quantitative results. Volatiles are reported in mol % and the 3-sigma detection limit for gases is about 0.3 ppm ($\sim 1 \times 10^{-15}$ mol) [17,18]. Precision and accuracy of seven capillary tubes with encapsulated atmosphere were N₂ (1.43, 0.05), O₂ (5.13, 0.05) and Ar (6.86, 4.60) relative percent, respectively. The gas results of the capillary tubes cluster close to the global atmospheric gas content, and they clearly demonstrate the robustness of the CFS-MS method for measuring gas in artificial and natural inclusions.

3. Results

The sylvite samples contain abundant fluid inclusions. They occur as planar arrays of primary inclusions parallel to crystal faces, where they are monophasic liquid, up to 5 microns size (Figure 1). There are also isolated inclusions with vapour bubbles, up to 50 microns in size (Figure 1), which implies entrapment of secondary inclusions by a recrystallization event during burial. The total volume of inclusions in the sylvite is composed of an approximately equal mixture of the arrays and the isolated inclusions. The halite samples similarly contain both planar arrays of inclusions and

isolated inclusions up to 70 microns, dominated by the planar arrays. Much of the sylvite is red, due to incorporation of the iron oxide haematite. This is a typical feature of sylvite worldwide [19,20]. The halite is predominantly white, and does not contain iron oxide.

The gas measurements showed that hydrogen was detected in all 13 sylvite samples and 2 of 10 halite samples. The mean hydrogen content for sylvite is 0.277%, and for halite is less than 0.001%.

The oxygen content for sylvite varies from 0% to 0.55%, and for halite varies from 0.04% to 0.37%.

Several sylvite samples contain measurable helium, especially in the samples containing the highest hydrogen contents (Figure 3, Table 1). In contrast, most of the halite samples contain no or negligible helium.

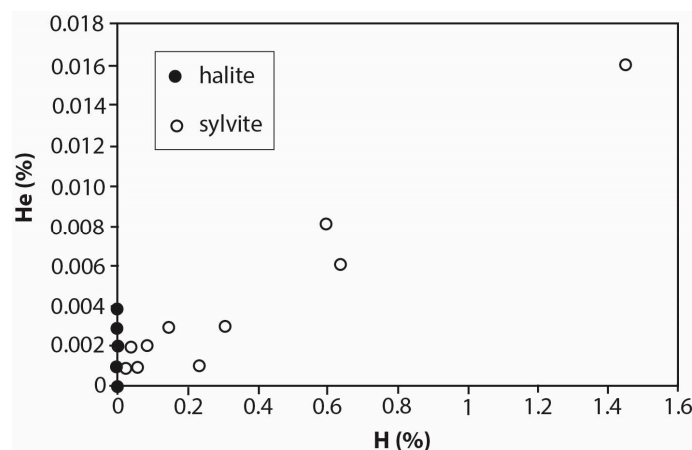


Figure 3. Cross-plot of concentrations of hydrogen (%) and helium (%) in volatiles released by cold-crushing of sylvite and halite samples (data in Table 1).

Table 1. Composition of volatiles released by cold-crushing samples of sylvite and halite from Boulby mine, and Eskdale No. 2 borehole.

Lab No.	Mineral	Crushes	Mine Panel	Total Gas (mols)	H ₂ (%)	He (%)	O (%)
140	sylvite	8		7.6×10^{-10}	0.028	0.002	0.089
186	sylvite	5		6.2×10^{-10}	0.018	0.001	0.055
187	sylvite	8		3.0×10^{-9}	0.023	0.001	0.055
188	sylvite	4		4.0×10^{-9}	0.045	0.001	0.096
189	sylvite	8		3.7×10^{-9}	0.028	0.001	0.553
194	sylvite	9	240	3.7×10^{-9}	0.303	0.003	0.111
195	sylvite	8	2008	2.1×10^{-9}	0.230	0.001	0.103
196	sylvite	10	240	4.0×10^{-9}	0.145	0.003	0
197	sylvite	10	2008	5.7×10^{-9}	0.633	0.006	0
281	sylvite	8		1.2×10^{-9}	0.020	0.001	0.278
283	sylvite	9		3.3×10^{-9}	0.080	0.002	0.278
287	sylvite	10	2008	5.6×10^{-9}	0.598	0.008	0.094
288	sylvite	10	2008	2.2×10^{-9}	1.451	0.016	0.186
146	halite	7		4.2×10^{-9}	0	0.001	0.039
190	halite	6		2.0×10^{-8}	0	0.003	0.065
191	halite	9		1.9×10^{-8}	0	0.004	0.201
192	halite	4	2001	2.5×10^{-11}	0	0	0.039
193	halite	6	2001	1.2×10^{-10}	0	0.001	0.206
263	halite	9	E2/4010ft	2.2×10^{-10}	0	0	0.16
264	halite	10	E2/3816ft	1.6×10^{-10}	0	0	0.373
265	halite	6	E2/3962ft	1.6×10^{-10}	0	0	0.119
271	halite	9	E2/3962ft	2.4×10^{-10}	0.005	0	0.348
282	halite	9		3.5×10^{-9}	0.001	0.002	0.104

The volatiles are dominated by water, and also include traces of argon, carbon dioxide and nitrogen detected by the CFS-MS method.

4. Discussion

4.1. Gas Composition

The occurrence of hydrogen in all of the sylvite samples is anomalous. Many samples of other rocks and minerals analysed in the same laboratory yield no hydrogen (not detected at 0.001% level). Most of the halite samples from the same setting at Boulby similarly yielded no detectable hydrogen. Accordingly, the mean value for hydrogen in the sylvite is far greater than for halite. The anomalous value for hydrogen is consistent with the prediction of hydrogen generation in the sylvite due to irradiation-induced radiolysis. The hydrogen content in the sylvite varies by two orders of magnitude, indicating significant sample heterogeneity, but is comparable with the variation found in other studies of hydrogen incorporation in minerals [9,21].

Experimental irradiation of halite crystals, where no natural source of irradiation is available, similarly generates hydrogen from radiolysis of fluid inclusion water [22,23]. The hydrogen is measurable despite the much shorter timescale of irradiation compared with that in a geological environment. This confirms that hydrogen from radiolysis should be expected within the fluid inclusions of potassium evaporite minerals.

Oxygen contents in the Boulby sylvite and halite do not show clear trends. Oxygen is routinely detected in the volatiles released from crushing samples, and is derived from a variety of sources including entrapped atmosphere [24,25]. Therefore, oxygen formed from radiolysis is not distinguishable against that from other, more abundant, sources. Similarly, argon formed by the decay of potassium in the sylvite is not distinguishable from that contributed by the atmosphere. Nitrogen, carbon dioxide and other components are similarly entrapped with the original water.

The highest helium contents occur in the samples with the highest hydrogen contents (Figure 3). Helium is another product of subsurface radioactivity, and a similar association between helium and hydrogen is recorded in the radioactive uranium-rich rocks of the Witwatersrand Basin, South Africa [6,26]. However, helium is a product of alpha irradiation from the uranium, and would not be a product of beta irradiation from potassium. Deposits of the Permian Zechstein sea, from which the sylvite was precipitated, are anomalously enriched in uranium [27,28]. This is especially evident on the European continent, but is also evident in north-east England, where modern groundwaters through Zechstein-age rocks have relatively high uranium contents [29]. Uranium is readily adsorbed into iron oxides such as haematite [30]. Thus, the widespread iron oxide in the Boulby sylvite may contain enough uranium to yield helium by alpha irradiation over a geological timescale. By contrast, the halite does not contain iron oxide, and concomitantly does not yield helium. The halite samples that contain no helium reflect the lack of a source of alpha irradiation in the halite, but some halite samples contain limited helium, which must have migrated from adjacent sylvite or another source of alpha irradiation. Some post-depositional fluid migration is implied by the entrapment of two-phase inclusions in the sylvite.

4.2. Subsurface Hydrogen

Radiolysis is one of several sources of hydrogen in the subsurface. Other mechanisms for hydrogen generation include serpentinization, oxidation of ferrous iron, and rock friction in seismogenic zones [6,9,31–33].

Hydrogen in the subsurface is important as a fuel for chemolithoautotrophy, i.e., simple life that does not depend upon photosynthesis. Chemolithoautotrophy may have been critical to the earliest development of life on Earth, and its importance in the subsurface today is becoming increasingly apparent [34–36]. Evidence for hydrogen generation therefore helps to ground-truth the mechanisms that could support such life.

Hydrogen formation by radiolysis may increase with elevated temperature [37]. However, the sylvite and halite sampled in this study have not been subject to very high temperatures. Estimates of thermal maturity using vitrinite reflectance in coal from the underlying Carboniferous rocks and the overlying Jurassic rocks of eastern England [38,39] suggest temperatures in the Permian section not much greater than 100 °C. The hydrogen has, therefore, been generated under diagenetic conditions rather than during the high temperatures and/or pressures of metamorphism.

Sylvite is less abundant than halite, as it requires a greater degree of evaporation of sea water. However, it is widely distributed in the geological record [40], and so could make a viable contribution to hydrogen generation in the crust. There is also much interest in possible mechanisms of hydrogen generation on other planets, because of its value to chemosynthetic life. Chloride minerals are widespread on Mars [41], and could include sylvite where chlorides are related to the weathering of basalt [42]. There are also indications of potassium evaporites on Mars [43], so the same process of hydrogen generation by radiolysis is likely to occur there.

5. Conclusions

The fluid inclusion volatile analysis technique has successfully detected traces of hydrogen in sylvite mineral samples. Hydrogen was detected in each of 13 sylvite samples, but in only negligible amounts or not at all in each of 10 halite samples from the same setting. These data are strongly consistent with a model in which irradiation from potassium in sylvite causes radiolysis of the water in fluid inclusions. The data indicate a mechanism by which hydrogen is generated in the subsurface, where it can be exploited by a chemoautotrophic deep biosphere.

Acknowledgments: We are grateful to J. Bowie and J. Still for skilled technical support and the staff at ICL-UK's Boulby mine (especially Thomas Edwards), STFC's Boulby underground Laboratory and the UK Centre for Astrobiology MINAR programme team (especially Sean Paling) for their support and supervised access to the site. The critical comments of two reviewers helped to improve the manuscript.

Author Contributions: John Parnell undertook the sampling. Nigel Blamey performed all analytical work. John Parnell wrote the manuscript.

Conflicts of Interest: The authors declare no conflict of interest.

References

1. Dubessy, J.; Pagel, M.; Beny, J.-M.; Christensen, H.; Hickel, B.; Kosztolanyi, C.; Poty, B. Radiolysis evidenced by H₂-O₂ and H₂-bearing fluid inclusions in three uranium deposits. *Geochim. Cosmochim. Acta* **1988**, *52*, 1155–1167. [[CrossRef](#)]
2. Savary, V.; Pagel, M. The effects of water radiolysis on local redox conditions in the Oklo, Gabon, natural fission reactors 10 and 16. *Geochim. Cosmochim. Acta* **1997**, *61*, 4479–4494. [[CrossRef](#)]
3. Nesmelova, Z.N.; Travnikova, L.G. Radiogenic gases in ancient salt deposits. *Geochem. Int.* **1973**, *5*, 554–559.
4. Smetannikov, A.F. Hydrogen generation during the radiolysis of crystallization water in carnallite and possible consequences of this process. *Geochem. Int.* **2011**, *49*, 916–924. [[CrossRef](#)]
5. Vovk, I.F. Radiolytic salt enrichment and brines in the crystalline basement of the East European Platform. In *Saline Water and Gases in Crystalline Basement*; Fritz, P., Frape, S.K., Eds.; Geological Association of Canada Special Paper: St. John's, NL, Canada, 1987; Volume 33, pp. 197–210.
6. Lin, L.H.; Hall, J.; Lippmann-Pipke, J.; Ward, J.A.; Sherwood Lollar, B.; DeFlaun, M.; Rothmel, R.; Moser, D.; Gihring, T.M.; Mislowack, B.; et al. Radiolytic H₂ in continental crust: Nuclear power for deep subsurface microbial communities. *Geochem. Geophys. Geosyst.* **2005**, *6*, Q07003. [[CrossRef](#)]
7. Parry, W.T.; Blamey, N.J.F. Fault fluid composition from fluid inclusion measurements, Laramide Age Uinta Thrust Fault, Utah. *Chem. Geol.* **2010**, *278*, 105–119. [[CrossRef](#)]
8. Blamey, N.J.F. Composition and evolution of crustal, geothermal and hydrothermal fluids interpreted using quantitative fluid inclusion gas analysis. *J. Geochem. Explor.* **2012**, *116–117*, 17–27. [[CrossRef](#)]
9. McMahon, S.; Parnell, J.; Blamey, N.J.F. Evidence for seismogenic hydrogen gas, a potential microbial energy source on Earth and Mars. *Astrobiology* **2016**, *16*, 690–702. [[CrossRef](#)] [[PubMed](#)]

10. Blair, C.C.; D'Hondt, S.; Spivack, A.J.; Kingsley, R.H. Radiolytic hydrogen and microbial respiration in subsurface sediments. *Astrobiology* **2007**, *7*, 951–970. [[CrossRef](#)] [[PubMed](#)]
11. Dzaugis, M.E.; Spivack, A.J.; Dunlea, A.G.; Murray, R.W.; D'Hondt, S. Radiolytic hydrogen production in the subseafloor basaltic aquifer. *Front. Microbiol.* **2016**, *7*, 76. [[CrossRef](#)] [[PubMed](#)]
12. Stewart, F.H. The petrology of the evaporites of the Eskdale No. 2 boring, east Yorkshire. *Mineral. Mag.* **1949**, *28*, 621–675. [[CrossRef](#)]
13. Woods, P.J.E. The geology of Boulby Mine. *Econ. Geol.* **1979**, *74*, 409–418. [[CrossRef](#)]
14. Talbot, C.J.; Tully, C.P.; Woods, P.J.E. The structural geology of Boulby (potash) mine, Cleveland, United Kingdom. *Tectonophysics* **1982**, *85*, 167–204. [[CrossRef](#)]
15. Cockell, C.S.; Payler, S.; Paling, S.; McLuckie, D. Boulby International Subsurface Astrobiology Laboratory. *Astron. Geophys.* **2013**, *54*, 2.25–2.27. [[CrossRef](#)]
16. Payler, S.J.; Biddle, J.F.; Coates, A.J.; Cousins, C.R.; Cross, R.E.; Cullen, D.C.; Downs, M.T.; Direito, S.O.L.; Edwards, T.; Gray, A.L.; et al. Planetary science and exploration in the deep subsurface: Results from the MINAR Program, Boulby Mine, UK. *Int. J. Astrobiol.* **2017**, in press. [[CrossRef](#)]
17. Blamey, N.J.F.; Parnell, J.; McMahon, S.M.; Mark, D.F.; Tomkinson, T.; Lee, M.; Shivak, J.; Izawa, M.R.M.; Banerjee, N.R.; Flemming, R.L. Evidence for methane in martian meteorites. *Nat. Commun.* **2015**, *6*, 7399. [[CrossRef](#)] [[PubMed](#)]
18. Norman, D.I.; Blamey, N.J.F. Quantitative gas analysis of fluid inclusion volatiles by a two mass spectrometer system. In *European Current Research on Fluid Inclusions*; No. XVI, Abstracts; University of Porto: Porto, Portugal, 2001; pp. 341–344.
19. Wardlaw, N.C. Carnallite-sylvite relationships in the Middle Devonian Prairie Evaporite Formation, Saskatchewan. *Geol. Soc. Am. Bull.* **1968**, *79*, 1273–1294. [[CrossRef](#)]
20. Garrett, D.E. *Potash Deposits, Processing, Properties and Uses*; Chapman & Hall: London, UK, 1996.
21. Parnell, J.; Boyce, A.J.; Blamey, N.J.F. Follow the methane: The search for a deep biosphere, and the case for sampling serpentinites, on Mars. *Int. J. Astrobiol.* **2010**, *9*, 193–200. [[CrossRef](#)]
22. Panno, S.V.; Czyscinski, K.V. Expected brine chemistry in a nuclear waste repository in salt. In *Proceedings of the First Canadian/American Conference on Hydrogeology: Practical Applications of Ground Water Geochemistry*, Banff, AL, Canada, 22–26 June 1984.
23. Gaudez, M.T.; Akram, N.; Toulhoat, P.; Toulhoat, N.; Palut, J.M. Analyses of radiolytic gases resulting from gamma irradiation of Asse rocksalt performed at Saclay. In *The Effects of Gamma Irradiation in Salt*; Celma, A.G., Ed.; Office for Official Publications of the European Communities: Luxembourg, 1996; pp. 209–256.
24. Blamey, N.J.F.; Boston, P.J.; Rosales-Lagarde, L. High-resolution signatures of oxygenation and microbiological activity in speleothem fluid inclusions. *Int. J. Speleol.* **2016**, *45*, 231–241. [[CrossRef](#)]
25. Blamey, N.J.F.; Brand, U.; Parnell, J.; Spear, N.; Benison, K.; Lécuyer, C.; Meng, F.; Ni, P. Paradigm shift in determining Neoproterozoic oxygen. *Geology* **2016**, *44*, 651–654. [[CrossRef](#)]
26. Ward, J.A.; Slater, G.F.; Moser, D.P.; Lin, L.H.; Lacrampe-Couloume, G.; Bonin, A.S.; Davidson, M.; Hall, J.A.; Mislouack, B.; Bellamy, R.E.S.; et al. Microbial hydrocarbon gases in the Witwatersrand Basin, South Africa: Implications for the deep biosphere. *Geochim. Cosmochim. Acta* **2004**, *68*, 3239–3250. [[CrossRef](#)]
27. Piestrzyński, A. Uranium and thorium in the Kupferschiefer formation, Lower Zechsten, Poland. *Miner. Depos.* **1990**, *25*, 146–151. [[CrossRef](#)]
28. Sun, Y.; Wang, J.; Li, S.; Jin, K.; Lin, M. Mechanism of uranium accumulation in the Kupferschiefer from Poland and Germany. *Energy Explor. Exploit.* **2005**, *23*, 463–473. [[CrossRef](#)]
29. Smedley, P.L.; Smith, B.; Abesser, C.; Lapworth, D. Uranium occurrences and behaviour in British groundwater. In *Groundwater Systems & Water Quality Programme Commissioned Report*; CR/06/050N; British Geological Survey: Nottingham, UK, 2006.
30. Duff, M.C.; Coughlin, J.U.; Hunter, D.B. Uranium co-precipitation with iron oxide minerals. *Geochim. Cosmochim. Acta* **2002**, *66*, 3533–3547. [[CrossRef](#)]
31. Sleep, N.H.; Bird, D.K. Niches of the pre-photosynthetic biosphere and geologic preservation of Earth's earliest ecology. *Geobiology* **2007**, *5*, 101–117. [[CrossRef](#)]
32. Sherwood Lollar, B.; Voglesonger, K.; Lin, L.-H.; Lacrampe-Couloume, G.; Telling, J.; Abrajano, T.A.; Onstott, T.C.; Pratt, L.M. Hydrogeologic controls on episodic H₂ release from Precambrian fractured—Energy for deep subsurface life on Earth and Mars. *Astrobiology* **2007**, *7*, 971–986. [[CrossRef](#)] [[PubMed](#)]

33. Hirose, T.; Kawagucci, S.; Suzuki, K. Mechanoradical H₂ generation during simulated faulting: Implications for an earthquake-driven subsurface biosphere. *Geophys. Res. Lett.* **2011**, *38*, L17303. [[CrossRef](#)]
34. Wankel, S.D.; Germanovich, L.N.; Lilley, M.D.; Genc, G.; DiPerna, C.J.; Bradley, A.S.; Olson, E.J.; Girguis, P.R. Influence of subsurface biosphere on geochemical fluxes from diffuse hydrothermal fluids. *Nat. Geosci.* **2011**, *4*, 461–468. [[CrossRef](#)]
35. Jones, A.A.; Bennett, P.C. Mineral microniches control the diversity of subsurface microbial populations. *Geomicrobiol. J.* **2014**, *31*, 246–261. [[CrossRef](#)]
36. Ishibashi, J.; Okino, K.; Sunamura, M. (Eds.) *Subseafloor Biosphere Linked to Hydrothermal Systems*; Springer: Tokyo, Japan, 2015.
37. Sterniczuk, M.; Bartels, D.M. Source of molecular hydrogen in high-temperature water radiolysis. *J. Phys. Chem. A* **2016**, *120*, 200–209. [[CrossRef](#)] [[PubMed](#)]
38. Bray, R.J.; Green, P.F.; Duddy, I.R. Thermal history reconstruction using apatite fission track analysis and vitrinite reflectance: A case study from the UK East Midlands and Southern North Sea. In *Exploration Britain: Geological Insights for the Next Decade*; Hardman, R.F.P., Ed.; Geological Society Special Publication: London, UK, 1992; Volume 67, pp. 3–25.
39. Słowakiewicz, M.; Tucker, M.E.; Vane, C.H.; Harding, R.; Collins, A.; Pancost, R.D. Shale-gas potential of the Mid-Carboniferous Bowland-Hodder Unit in the Cleveland Basin (Yorkshire), Central Britain. *J. Pet. Geol.* **2015**, *38*, 59–76. [[CrossRef](#)]
40. Warren, J.K. Evaporites through time: Tectonic, climatic and eustatic controls in marine and nonmarine deposits. *Earth Sci. Rev.* **2010**, *98*, 217–268. [[CrossRef](#)]
41. Osterloo, M.M.; Hamilton, V.E.; Bandfield, J.L.; Glotch, T.D.; Baldrige, A.M.; Christensen, P.R.; Tornabene, L.L.; Anderson, F.S. Chloride-bearing materials in the Southern Highlands of Mars. *Science* **2008**, *319*, 1651–1654. [[CrossRef](#)] [[PubMed](#)]
42. Tosca, N.J.; McLennan, S.M. Chemical divides and evaporite assemblages on Mars. *Earth Planet. Sci. Lett.* **2006**, *241*, 21–31. [[CrossRef](#)]
43. Elwood Madden, M.E.; Bodnar, R.J.; Rimstidt, J.D. Jarosite as an indicator of water-limited chemical weathering on Mars. *Nature* **2004**, *431*, 821–823. [[CrossRef](#)] [[PubMed](#)]



© 2017 by the authors. Licensee MDPI, Basel, Switzerland. This article is an open access article distributed under the terms and conditions of the Creative Commons Attribution (CC BY) license (<http://creativecommons.org/licenses/by/4.0/>).